Pointwise Assessment of Three-dimensional Computer Reconstruction of Mitral Leaflet Surfaces from Rotationally Scanned Echocardiograms in Vitro

Gerard Bashein, MD, PhD, Malcolm E. Legget, MB, ChB, and Paul R. Detmer, PhD,
Seattle and Bothell, Washington; and Auckland, New Zealand

Three-dimensional transesophageal echocardiography offers promise for improved understanding of mitral leaflet pathology, but it has not been validated quantitatively, nor has the minimum number of imaging planes for satisfactory reconstruction been determined with a rotational scanning geometry. This study assessed its accuracy in vitro by comparing, on a 1 × 1-mm grid, the surfaces of mitral leaflets derived from 5-degree rotational ultrasonic scans with those derived from laser scans of casts of the atrial side of the leaflets. Overall, the ultrasonically derived surface had a mean absolute deviation of 0.65 ± 0.12 mm from the laser-derived surface. Using only alternate imaging planes (10-degree increments) made no significant difference in the overall distribution of deviations ($P = .56$), although the distributions on some individual specimens differed markedly. We conclude that 5-degree rotational scanning in vitro can reconstruct the mitral valve leaflets with sufficient accuracy and detail to render clinically important features. (J Am Soc Echocardiogr 2004;17:239-46.)

Three-dimensional (3D) echocardiography offers great promise for improving the understanding of mitral leaflet pathology,[1] planning operations,[2,3] and assessing surgical results.[2,4] However, to date the reports evaluating the technique have been mostly qualitative,[5,6] semiquantitative,[7] or indirect quantitative comparisons.[8-11] The technique has not undergone rigorous quantitative evaluation, nor has it been determined what spatial sampling density is necessary to make a satisfactory 3D reconstruction. The possible in vivo imaging methods for validation of 3D reconstruction of the mitral leaflets, fast computed tomography and magnetic resonance imaging, have spatial resolution that is inferior to that of ultrasound, making them unsuitable for comparison. Therefore, we designed an in vitro study to simulate transesophageal rotational scanning and then to compare the surface reconstructions of the mitral leaflets from ultrasonic scans taken at 5- and 10-degree increments with laser scans of casts of the atrial surfaces of the leaflets.

From the University of Washington, Seattle, Washington (G.B.); Green Lane Hospital, Auckland, New Zealand (G.B., M.E.L.); and Philips Ultrasound, Bothell, Washington (P.R.D.).

Supported in part by a sabbatical leave from the University of Washington, Seattle (G.B.). Philips Ultrasound provided the Silicon Graphics computer, transesophageal probe, and software to reconfigure the HDI 5000CV ultrasound system into the research mode, acquire data automatically, and perform scan conversion offline.

Reprint requests: Gerard Bashein, MD, PhD, Department of Anesthesiology, Box 356540, University of Washington, Seattle, WA 98195-6540 (E-mail: *gb@u.washington.edu*).

0894-7317/$30.00

doi:10.1067/j.echo.2003.11.016

METHODS

Pig hearts were obtained fresh from the processing line of a local abattoir and kept frozen until ready for use. The preparation of the hearts proceeded as follows: the ascending aorta was transected immediately proximal to the innominate artery and the leaflets of the aortic valve were excised from within the aortic lumen. To enable retrograde filling of the left ventricular cavity from the aorta, a 12.7 mm–diameter tubing connector was inserted into the ascending aorta, and a watertight seal was made with nylon cable clamps. The coronary arteries were ligated with silk suture.

To simulate the normal distension of the mitral leaflets during systole, the left ventricular cavity was filled with a plastic material, either silicone rubber compound (RTV11, General Electric Co, Waterford, NY) or hydrophilic polysiloxane dental impression material (Reprosil, Dentsply International Inc, Milford, Del), and then pressurized by the aortic root with a column of water about 2-m high. To obtain varying valve geometries, a few primary or secondary chordae of either leaflet were cut arbitrarily in most specimens.

After the plastic material cured, the left atrial walls were excised, leaving a rim of tissue of less than 1 cm around the mitral annuli. Plastic material that

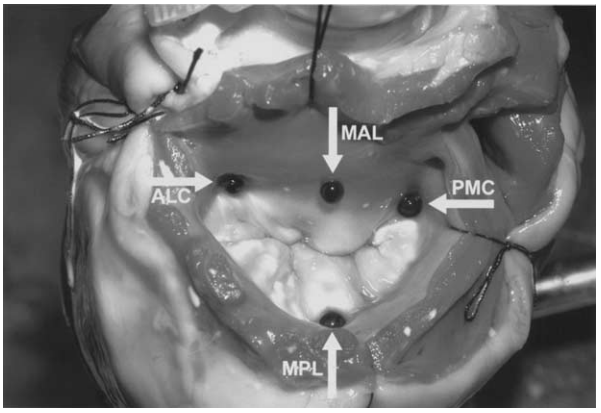

Figure 1 Photograph of a prepared porcine heart, showing unroofed left atrium and closed mitral leaflets. Four glass-headed dressmaker's pins (*arrows*) are positioned near midanterior leaflet (*MAL*) and midposterior leaflet (*MPL*), and anterolateral commissure (*ALC*) and posteromedial commissure (*PMC*).

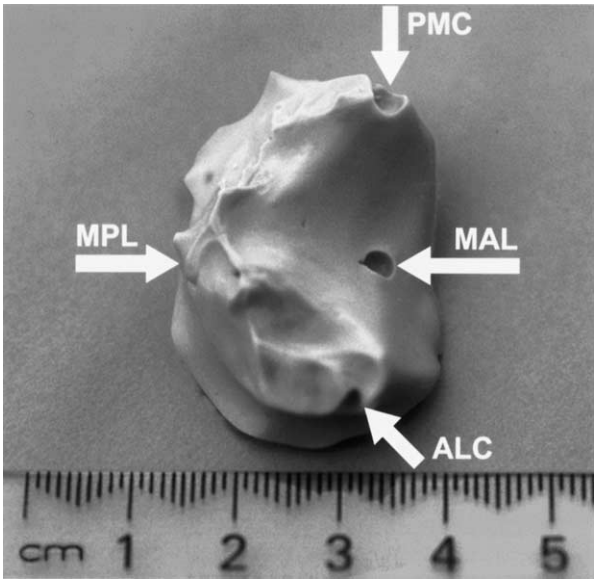

Figure 2 Photograph of atrial cast made from the heart shown in Figure 1. Midposterior leaflet (*MPL*) indentation is out of view on left side of image. *Arrows* are indentations of fiducial pinheads. *ALC*, Anterolateral commissure; *MAL*, midanterior leaflet; *PMC*, posteromedial commissure.

had extruded into the atrium because of valvular incompetence was trimmed with a scalpel to the level of the surface of the leaflets. Dressmaker's pins having 3 mm–diameter glass heads were inserted into the annulus at the approximate midpoint of the anterior and posterior leaflets and at the anterolateral and posteromedial commissures to serve as fiducial marks for registering the ultrasonically and optically scanned images (Figure 1).

Ultrasonic imaging was performed in a bath of 4.62% saline solution at a controlled room temperature of 22°C, giving the speed of sound[12] for which the ultrasound system was calibrated (1540 m/s). A jig held the heart in position for imaging within the bath, and another jig having a flexible arm held the transducer end of a 5.5-MHz multiplane transesophageal ultrasonic probe (MPT7-4, Philips Medical Systems, Bothell, Wash). Imaging was performed from an atrial viewpoint at a distance of about 5 cm, with the sector centered near the middle of the line of coaptation, to simulate in vivo imaging in human beings. A soft artist's brush was used to remove adherent air bubbles from the surface of the mitral leaflets.

Using special software supplied by the manufacturer, the ultrasound instrument (HDI 5000CV, Philips Medical Systems) was reconfigured into a research mode. This mode enabled automatic acquisition of rotationally scanned data at 5-degree angular increments with (simulated) electrocardiographic gating. The data in each imaging plane were acquired in polar (r, θ) form and downloaded into a networked computer (Model O2, Silicon Graphics, Mountain View, Calif). Immediately upon completing the ultrasonic imaging for each heart, a cast of the atrial side of mitral leaflets was made using dental impression material (Figure 2).

Offline scan conversion was performed using proprietary software (Philips Medical Systems) to generate spatially registered sets of 2-dimensional (2D) images (256 × 384 pixels) for each heart. The images were then loaded into another custom software package for image segmentation, 3D viewing, and editing.[13] This software incorporates a scientific visualization package (AVS, Version 5.4, Advanced Visual Systems, Waltham, Mass) to display the segmented structures.

Using the leading-edge method, the surface of the mitral leaflets and the heads of the 4 fiducial pins were traced manually, without referring to the leaflet casts. The leaflets were outlined as a single structure; no attempt was made to identify the line of coaptation. The outlining program generated Bezier curves to represent the intersection of the leaflet surface with each imaging plane, and this was resampled to form the final leaflet data set. The location of the center of each (spherical) pinhead fiducial was determined by projecting along the ultrasound beam 1.5-mm deep (the pinhead's radius) to the point closest to the transducer in the 2D slice having the brightest image of each fiducial.

The software placed the fiducial marks and leaflet outline data points into a common 3D coordinate system, referenced to the face of the transesophageal probe. The origin of the coordinate system was taken to be the common apex point of the imaging

sectors, with the z-coordinate collinear with the rotational axis of the ultrasonic array and oriented in the direction of the central transmitted ultrasonic beam. The x-axis was aligned along the transducer array when it was set to the 0-degree position, and the y-axis was oriented to form a right-hand coordinate system (See inset, Figure 3).

Data for reconstructing 3D surfaces of the leaflet casts were acquired by laser scanning with a handheld probe for which the position and orientation in 3D space were measured with a magnetic tracking device (Polhemus Fastscan, Applied Research Associates NZ Ltd, Christchurch, New Zealand). The scanner has a manufacturer-specified maximum error tolerance of ±1 mm at the range used in this study. The surface of each cast was formed from its cloud of 3D data points by radial basis function interpolation software (FastRBF, Applied Research Associates NZ Ltd) running within a mathematical software package (Matlab, Version 6.1, Mathworks, Natick, Mass). The software also enabled manual identification of the 3D location of the center of the recess made by each fiducial pinhead in the cast. These data were stored in computer files for subsequent matching with the corresponding ultrasonic representations.

Comparison between the ultrasonic- and laser-reconstructed surfaces was performed with custom software written for this study in the aforementioned mathematical software package (Matlab). Rigid body registration was performed by a least squares method[14] as follows: first, the centroid of the 4 laser fiducials was translated to coincide with the centroid of the 4 ultrasound fiducials. Next, the rotational transformation was calculated that (in a least squares sense) best aligned the homologous laser and ultrasonic fiducials.[15] The resulting coordinate transformation was then used to place all of the laser data into the ultrasonic coordinate system for the purpose of subsequent analysis and comparison.

With 3D rotational scanning, the data density is much greater near the center of rotation; hence, a point-by-point comparison of the raw ultrasonic data with the laser-generated surface would place undue emphasis on the center of the scan. To mitigate this effect, a 1 × 1-mm rectilinear grid was constructed in the x-y plane, covering the convex hull of the ultrasonic surface data. Next, to determine the z-coordinate values at each node in the grid, a series of cubic interpolations were performed on the basis of Delaunay triangulation of the data using subroutines supplied with Matlab. Wire frame models of the ultrasonically determined leaflet surface were then constructed over the grid. The same cubic interpolation subroutines were used to calculate the z-coordinates of the laser surface, transformed into the ultrasonic coordinate system and evaluated at all

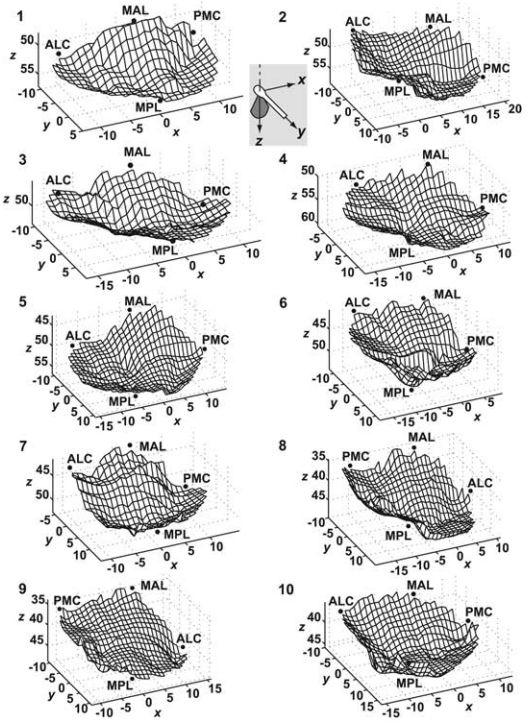

Figure 3 Composite of perspective drawings, from atrial viewpoint, of ultrasonically determined wire mesh reconstruction of 10 mitral leaflets. Origin of coordinate system is located at rotational center of face of transducer as shown in *inset* between leaflet Nos. 1 and 2. All dimensions are in millimeters. Hidden lines have been removed. Fiducial marks are indicated with *bullets*. *ALC*, Anterolateral commissure; *MAL*, midanterior leaflet; *MPL*, midposterior leaflet; *PMC*, posteromedial commissure.

nodes of the ultrasonic grid. The fit between the ultrasonic and laser representations of the leaflet surfaces was assessed as the differences between the laser and ultrasonic z-coordinate values over all the grid nodes defining each leaflet. Descriptive statistics, box plots, and the dependency of fit on rotational angle and radial distance from the intersection of the mitral surface with the ultrasound acquisition axis of rotation were calculated for these distributions.

Data are shown as mean ± SD. Statistical calculations were made using the statistics toolbox in the computer program (Matlab, Version 6.1, Mathworks) for the Kolmogorov-Smirnov test and box plots, and separate software (JMP, Release 5.0.1a, SAS Institute, Cary, NC) for all other tests. Two-sided P values $< .05$ were considered significant.

RESULTS

Ten hearts had a weight of 344.0 ± 38.5 g and mitral valve area of 436 ± 82 mm^2. The time required to manually trace the outlines was about 1.5 hours per specimen. The number of raw ultrasound data

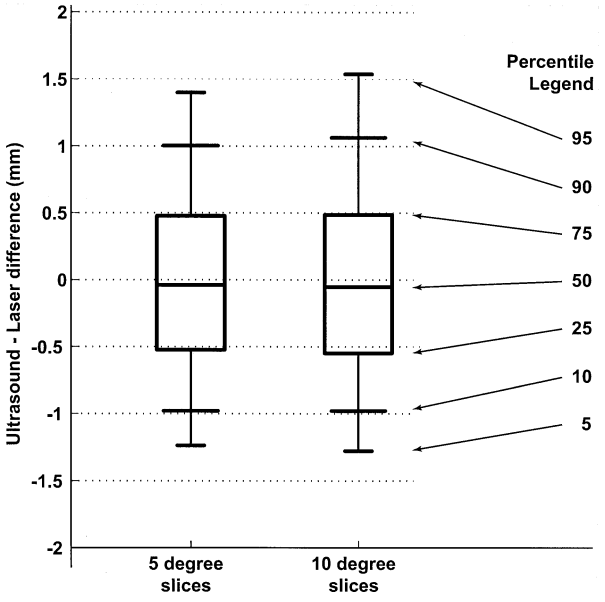

Figure 4 Box and whisker plots of pooled deviations in z-dimension between laser- and ultrasound-interpolated data at 1-mm grid points for 5- and 10-degree slices. Data have been normalized to 0 mean. Legend for percentiles represented by each *crossbar* is shown along right-hand box plot.

points per heart was 1194 ± 490, and the number of laser data points was 4576 ± 390. The mean fiducial registration error between the ultrasound and laser representations of the pinheads (for 40 points, or 4 points/heart) was 0.88 ± 0.38 mm.

The ultrasonic reconstructions of all of the leaflets on a 1 × 1-mm grid are shown in an atrial perspective view in Figure 3, with the locations of the fiducial marks indicated with bullets. Because the retained rim of atrial tissue was subject to being displaced in the saline bath, and because the ventricular surfaces of the leaflets were tightly applied to the material filling the left ventricle, the exact position of the annulus was difficult to identify in some of the ultrasonic images. This required trimming of the ultrasonic data peripherally where it extended beyond the laser-defined annulus.

Box and whisker plots of the residual errors (Z-dimension, Figure 3) between laser and ultrasound surfaces at grid points are shown in Figure 4 for the pooled data. The distributions of the residuals for reconstructions made with 5-degree angular increments did not differ significantly from those made with 10-degree increments ($P = .56$, Kolmogorov-Smirnov goodness of fit test). Similarly, the mean of the absolute deviation (AD) between all ultrasound- and laser-fitted surfaces for 5-degree slices (n = 4351) was 0.65 ± 0.12 mm, and for 10-degree slices (n = 8529, with 2 surfaces per specimen) was 0.64 ± 0.12 mm ($P = .68$, Wilcoxon rank sum test).

Polynomial regression to determine the dependency of the AD (in millimeters) on radial distance from the center of rotation of the image planes (R, in millimeters) found significant terms of only up to second order:

$$AD = 0.501 + 0.019R - 0.0013\ (R - 8.88)^2;$$
$$AD = 0.473 + 0.020R - 0.0011\ (R - 8.80)^2;$$

$r^2 = 0.014$, $p < 0.001$, for 5° data; and
$r^2 = 0.017$, $p < 0.001$, for 10° data.

Regression revealed no significant dependency of the AD on the angle of transducer rotation with respect to the intercommissural line.

Box plots of the deviations for individual specimens are shown in Figure 5. For some specimens (ie, hearts numbered 4, 9, and 10), important differences are apparent between the 5- and 10-degree data for the even- and odd-numbered slices. The large differences tended to occur near the poorly defined annuli and where the ultrasound beam intersected the leaflet nearly tangentially in regions of steep curvature. This is illustrated by example in Figure 6.

DISCUSSION

Characterizing the alterations in mitral valve geometry because of intrinsic valve disease or ischemic or nonischemic cardiomyopathy depends on having an accurate pointwise description of the leaflet surface. For example, the shape of the mitral leaflet and annulus has been shown to affect leaflet stress,[16,17] which may be implicated in the long-term failures of valve repair as a result of disruptions of leaflet, chordal, or annular sutures.[18] Quantitatively accurate 3D models of the mitral leaflet may also be useful to provide boundary conditions for finite element models of leaflet stress[19,20] and to assess proposed new operations for the treatment of mitral regurgitation.[20,21]

To our knowledge, this is the first study to make a registered, point-by-point comparison of the ultrasonically derived reconstruction of the surface of the mitral leaflet with a separate reference standard. The accuracy of the results may have been limited by the fact that a cast, rather than the leaflet itself, was scanned by the laser system, which has a manufacturer-specified error of ±1 mm at the range used in this study. This error is comparable with the 0.88- ± 0.38-mm mean fiducial point registration error that we encountered and the mean AD of about 0.65 mm between the ultrasound and laser surfaces.

Previous studies validating 3D computer modeling from echocardiographic data have mainly used summary measures (surface area or volume) to compare 3D reconstructions,[22,23] and it is well

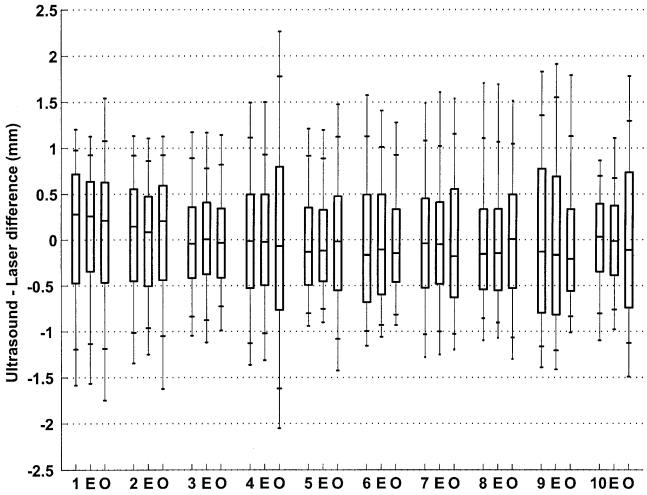

Figure 5 Triples of box and whisker plots for each heart specimen, of similar construction to those in Figure 4. *First plot* in each triple carries specimen number, which corresponds to number of each reconstruction in Figure 3 and represents the full 5-degree data set for that specimen. *Second and third plots* represent reconstructions from 10-degree data, using even-numbered (*E*) and odd-numbered (*O*) slices, respectively.

known that such metrics tend to average out errors in the individual surface data points, making for favorable comparisons in the face of some major localized discrepancies between the fitted surfaces. Comparing linear rather than surface or volume measures may be a more demanding test of the methodology. For example, Binder et al[24] compared the longest dimension of ultrasonically derived models of balloon phantoms and liver specimens imaged in a water tank and found a mean error of 0.3 mm with a SD of 1.6 mm.

In fitting a surface, a mean error toward or away from the transducer (z-direction in this study) is of no importance, because it merely represents a translation of the surface and not a change in its contour. However, the AD of the derived surface from the reference surface may have diagnostic importance. Overall, this study found a mean AD of about 0.65 mm between the ultrasonic- and laser-reconstructed surfaces using data taken at either 5- or 10-degree increments.

This study used simulated electrocardiographic gating to acquire 3D ultrasound data automatically by rotating the transducer array and recording another 2D image after each trigger. During in vivo imaging, the time needed to rotate the array is typically less than 5% of the cardiac cycle, and, if systole were the only period of interest, a new imaging plane could be acquired with each heart beat. At a heart rate of 60 bpm and using 5-degree increments, it would take 36 seconds to acquire image data from 0 to 175 degrees. This probably represents a practical limit to the time that mechanical ventilation could be suspended to acquire data in an intraoperative situation. With a patient spontaneously breathing, it would be desirable for the breath to be held for a shorter time. Respiratory gating could be used to take more images over several short, held breaths. However, it is not known how closely a patient can breathe to the same lung volume (and heart position) repeatedly and how much additional registration error would be introduced by acquiring data during more than 1 breath. The new 2D-array ultrasound imaging technology would eliminate the need for triggered acquisitions if the field of view were kept sufficiently small and imaging depth were not excessive. Even when triggered acquisitions are required using 2D arrays, the number of cardiac cycles needed to cover the desired volume of tissue will be less than what is required with a mechanical system.

Surprisingly, our results show that taking data in 10-degree, rather than 5-degree, increments does not result in significantly different overall accuracy in terms of the mean AD between the ultrasound- and laser-reconstructed leaflet surfaces or in the distribution of the deviations at individual grid points. Nevertheless, some specimens exhibited significant loss of accuracy on 10-degree scans (Figure 5). Thus, it appears that valves having only minor distortion can be adequately reconstructed from 10-degree slices, but that valves having major anatomic abnormalities require 5-degree or finer sampling.

Regression analysis showed that, overall, the mean AD between the surfaces varied in a quadratic manner with radial distance from the axis of transducer rotation, for both the 5- and 10-degree data sets, with the maximum value occurring near the middle of the range of radii. This suggests that the

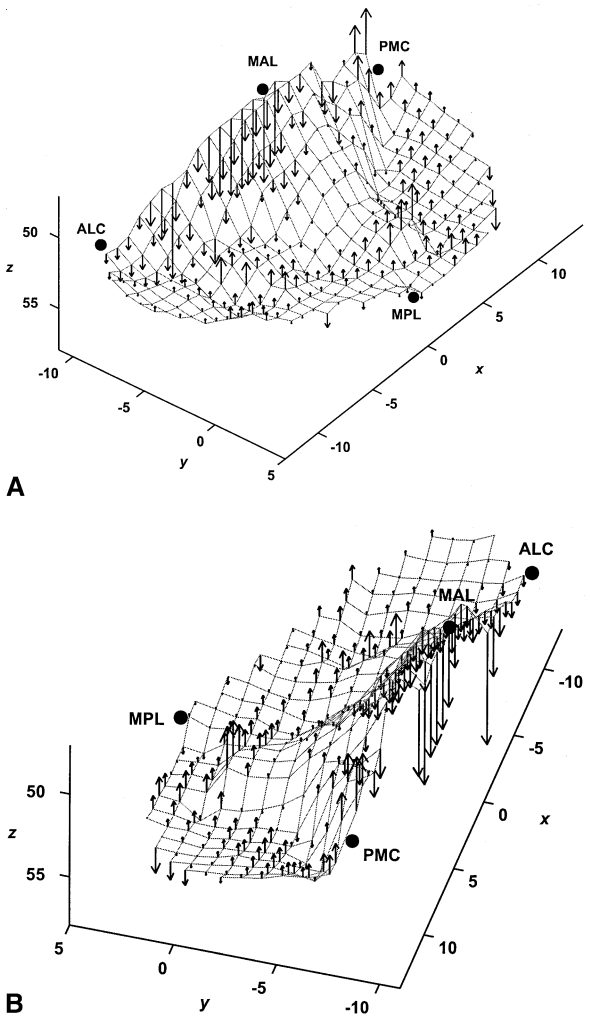

Figure 6 Wire mesh drawings of ultrasonic reconstruction of specimen No. 1 with residuals between ultrasonic and laser surface shown with *arrows* drawn to same scale as mesh. *Arrows* are not shown at those mesh points having too small a residual to be represented graphically. Mean absolute deviation of 275 mesh points in this specimen is 0.83 mm, and 95th percentile is 1.94 mm. **A**, Atrial viewpoint similar to that in Figure 3, but without hidden line removal. **B**, View from anterior atrial side, showing that very large residuals are confined to annular edge of anterior leaflet. All 13 points that exceed 95th percentile are located along anterior annular border and likely represent artifacts of misregistration with the laser reconstruction. *ALC*, Anterolateral commissure; *MAL*, midanterior leaflet; *MPL*, midposterior leaflet; *PMC*, posteriomedial commissure.

increase in ultrasonic beam width that occurs with increasing distance off the axis of the sector is not the major factor limiting the reconstruction accuracy, but that the irregularities of the surface of the leaflets are greatest in the region midway between the center of the valve and the annulus. In addition, regression analysis did not find any dependency of the deviations between the ultrasonic and laser data on the transducer rotation angle. Overall, the expected deviation was within 1 mm over the entire range of data.

Previously reported studies of rotational transesophageal scanning of the mitral valve have used angular increments ranging from 2 degrees[4] to 20 degrees.[25] Analysis of the out-of-plane beam width for this (typical) transesophageal probe confirms that 5-degree increments should enable as accurate a reconstruction of the mitral leaflet as finer increments would. For example, the distance between the image planes using a 5-degree increment would be 0.9 mm at a 10-mm radial distance from the central axis of rotation and 1.3 mm at a 15-mm distance. The elevation thickness of a phased-array ultrasound beam (measured as the half-power width) is determined by the diffraction limit of the array aperture and the fixed focus lens used to set the imaging depth of field. Elevation thickness varies with depth and is never smaller than about 2 mm for this scanhead. Thus, at the outermost extremes of a 30-mm diameter valve, smaller angular increments would provide only marginal improvement in surface sampling.

Limitations

Performing this study in vitro, without motion, eliminated any errors as a result of respiration, leaflet vibration, beat-to-beat variation in cardiac motion, and the temporal misregistration that would occur when acquiring images asynchronously during a series of heartbeats. By contrast, the mitral annulus was indistinct in this in vitro preparation, and, were movement present, the annulus would have been more clearly identified as the hinge point. In vivo, the annulus could be modeled separately,[26] and that model could then be used to tether the boundaries of the leaflet model.

Filling the ventricular cavity with a plastic material altered the acoustical interface with the leaflets, and the lack of crisp outlines from echo-free blood pools on both sides of the leaflet no doubt added error in tracing the leaflet surfaces. The strong reflections generated by the plastic material made the leaflet surface more difficult to locate precisely in regions oriented obliquely to the ultrasonic beam. How in vivo studies might be similarly affected if the leaflets were calcified, fibrosed, or otherwise made echodense is unclear.

Finally, whereas we were able to cut chordae to produce distorted leaflet geometry for purposes of comparison, we could not use the specimens in which large amounts of regurgitation occurred, because under those conditions it was impossible to maintain pressurization of the ventricle for a long enough time to allow the plastic material to cure.

Manual image segmentation requires about 1.5 hours per heart with our system, so routine clinical application of surface rendering of the mitral leaflets must await development of fast and reliable automated recognition of the leaflet surfaces in each slice. Early efforts at automated recognition have been encouraging,[27] probably because the outline of the mitral leaflet is more distinct than that of the endocardial border, which has been the major thrust of research in automatic border outlining thus far.

Conclusion

Three-dimensional rotational scanning at 5-degree increments enables accurate modeling of mitral leaflet surfaces in vitro. Overall, the mean AD between the ultrasound- and laser-fitted surfaces (0.65 mm) is comparable with the advertised error in the laser instrument itself (±1 mm) and to the mean registration error between the 4 fiducial points of each specimen (0.88 mm). Overall, eliminating alternate imaging planes to give 10-degree rotational increments did not change the mean AD or the distribution of deviations, but it did produce large errors in some specimens, which might be significant if reconstructions were made clinically. The methodology used in this study may also be applicable to evaluate mitral leaflet imaging by the new real-time 2D echocardiographic instruments.

The authors wish to thank Prof Norman Sharpe, Department of Medicine, Auckland Hospital, Auckland, New Zealand, for providing use of the echocardiographic laboratory for imaging; Richard Fright, Applied Research Associates, Christchurch, New Zealand, for making the laser scans; Edward Bolson, Cardiovascular Research Laboratory, University of Washington, Seattle, Washington, for programming the image segmentation software and providing assistance in its use; John Bodley, Department of Engineering Science, University of Auckland, for programming assistance with data reduction; Grant Christie, Systematic Solutions Ltd, Auckland, for advice on making valve casts; and Paul Couper, Philips Ultrasound, Auckland, for engineering assistance.

REFERENCES

1. Sutaria N, Northridge D, Masani N, Pandian N. Three dimensional echocardiography for the assessment of mitral valve disease. Heart 2000;84:7-10.
2. De Castro S, Salandin V, Cartoni D, Valfre C, Salvador L, Magni G, et al. Qualitative and quantitative evaluation of mitral valve morphology by intraoperative volume-rendered three-dimensional echocardiography. J Heart Valve Dis 2002; 11:173-80.
3. Patel AR, Mochizuki Y, Yao J, Pandian NG. Mitral regurgitation: comprehensive assessment by echocardiography. Echocardiography 2000;17:275-83.
4. Acar P, Laskari C, Rhodes J, Pandian N, Warner K, Marx G. Three-dimensional echocardiographic analysis of valve anatomy as a determinant of mitral regurgitation after surgery for atrioventricular septal defects. Am J Cardiol 1999;83:745-9.
5. Godoy IE, Bednarz J, Sugeng L, Mor-Avi V, Spencer KT, Lang RM. Three-dimensional echocardiography in adult patients: comparison between transthoracic and transesophageal reconstructions. J Am Soc Echocardiogr 1999;12:1045-52.
6. Hozumi T, Yoshikawa J, Yoshida K, Akasaka T, Takagi T, Yamamuro A. Assessment of flail mitral leaflets by dynamic three-dimensional echocardiographic imaging. Am J Cardiol 1997;79:223-5.
7. Salustri A, Becker AE, van Herwerden L, Vletter WB, Ten Cate FJ, Roelandt JR. Three-dimensional echocardiography of normal and pathologic mitral valve: a comparison with two-dimensional transesophageal echocardiography. J Am Coll Cardiol 1996;27:1502-10.
8. Chauvel C, Bogino E, Clerc P, Fernandez G, Vernhet JC, Becat A, et al. Usefulness of three-dimensional echocardiography for the evaluation of mitral valve prolapse: an intraoperative study. J Heart Valve Dis 2000;9:341-9.
9. Breburda CS, Griffin BP, Pu M, Rodriguez L, Cosgrove DM III, Thomas JD. Three-dimensional echocardiographic planimetry of maximal regurgitant orifice area in myxomatous mitral regurgitation: intraoperative comparison with proximal flow convergence. J Am Coll Cardiol 1998;32:432-7.
10. Lange A, Palka P, Donnelly J, Burstow D. Quantification of mitral regurgitation orifice area by 3-dimensional echocardiography: comparison with effective regurgitant orifice area by PISA method and proximal regurgitant jet diameter. Int J Cardiol 2002;86:87-98.
11. Chen Q, Nosir YF, Vletter WB, Kint PP, Salustri A, Roelandt JR. Accurate assessment of mitral valve area in patients with mitral stenosis by three-dimensional echocardiography. J Am Soc Echocardiogr 1997;10:133-40.
12. Urick RJ. Principles of underwater sound. 2nd ed. New York: McGraw-Hill; 1975. p. 106.
13. Sheehan FH, Bolson EL, Martin RW, Bashein G, McDonald J. Quantitative three-dimensional echocardiography: methodology, validation, and clinical applications. In: Wells WM, Colchester A, Delp S, editors. Medical image computing and computer assisted intervention MICCAI'98: first international conference. Berlin: Springer Verlag; 1998. p. 102-9.
14. Fitzpatrick JM, West JB, Maurer CR Jr. Predicting error in rigid-body point-based registration. IEEE Trans Med Imaging 1998;17:694-702.
15. Arun KS, Huang TS, Blostein SD. Least-squares fitting of two 3-D point sets. IEEE Trans Pattern Analysis Machine Intell 1987;9:698-700.
16. Salgo IS, Gorman JH III, Gorman RC, Jackson BM, Bowen FW, Plappert T, et al. Effect of annular shape on leaflet curvature in reducing mitral leaflet stress. Circulation 2002; 106:711-7.
17. Arts T, Meerbaum S, Reneman R, Corday E. Stresses in the closed mitral valve: a model study. J Biomech 1983;16:539-47.
18. Gillinov AM, Cosgrove DM, Blackstone EH, Diaz R, Arnold JH, Lytle BW, et al. Durability of mitral valve repair for degenerative disease. J Thorac Cardiovasc Surg 1998;116: 734-43.
19. Kunzelman KS, Reimink MS, Cochran RP. Annular dilatation increases stress in the mitral valve and delays coaptation: a finite element computer model. Cardiovasc Surg 1997;5:427-34.

20. Votta E, Maisano F, Soncini M, Redaelli A, Montevecchi FM, Alfieri O. Three-dimensional computational analysis of the stress distribution on the leaflets after edge-to-edge repair of mitral regurgitation. J Heart Valve Dis 2002;11:810-22.
21. Messas E, Guerrero JL, Handschumacher MD, Conrad C, Chow CM, Sullivan S, et al. Chordal cutting: a new therapeutic approach for ischemic mitral regurgitation. Circulation 2001;104:1958-63.
22. Siu SC, Rivera JM, Guerrero JL, Handschumacher MD, Lethor JP, Weyman AE, et al. Three-dimensional echocardiography: in vivo validation for left ventricular volume and function. Circulation 1993;88:1715-23.
23. Siu SC, Rivera JM, Handschumacher MD, Weyman AE, Levine RA, Picard MH. Three-dimensional echocardiography: the influence of number of component images on accuracy of left ventricular volume quantitation. J Am Soc Echocardiogr 1996;9:147-55.
24. Binder TM, Moertl D, Mundigler G, Rehak G, Franke M, Delle-Karth G, et al. Stereolithographic biomodeling to create tangible hard copies of cardiac structures from echocardiographic data: in vitro and in vivo validation. J Am Coll Cardiol 2000;35:230-7.
25. George SJ, Al-Ruzzeh S, Amrani M. Mitral annulus distortion during beating heart surgery: a potential cause for hemodynamic disturbance–a three-dimensional echocardiography reconstruction study. Ann Thorac Surg 2002;73:1424-30.
26. Legget ME, Bashein G, McDonald JA, Munt BI, Martin RW, Otto CM, et al. Three-dimensional measurement of the mitral annulus by multiplane transesophageal echocardiography: in vitro validation and in vivo demonstration. J Am Soc Echocardiogr 1998;11:188-200.
27. Mikic I, Krucinski S, Thomas JD. Segmentation and tracking in echocardiographic sequences: active contours guided by optical flow estimates. IEEE Trans Med Imaging 1998;17:274-84.